Now you see it, now you don't: radial trace filtering tutorial

David C. Henley

ABSTRACT

The radial trace domain has been shown to be useful for modeling and attenuating source-generated coherent noise on raw seismic trace gathers. While the general principles are well-known, some of the variations of the method are not, and the details of the analysis and design process have never been explicitly outlined. We demonstrate here a general strategy for analyzing coherent noise on input gathers and designing a filter sequence for removal of the noise. The strategy is a subjective one, and it relies on the judgement of the processor at every step to determine how much filtering is "enough". The process is illustrated with screen-captured ProMAX processing flows, as well as pre- and post-processing images of trace gathers. We give recommendations for parameter selection and show an overall processing flow, explaining the presence of each ProMAX module. We also show the details for two 'specialty' coherent noise attenuation methods utilizing the radial trace domain.

INTRODUCTION

Soon after introducing the radial trace transform, Claerbout (1983) showed that it was capable of separating ground roll from reflections on seismic trace gathers. The fan geometry of the sampling trajectories of the radial trace (R-T) transform fits the pattern of source-generated linear noise wavefronts which intersect the source (or receiver) origin on the original gather. Hence, individual noise trains are efficiently represented in the R-T domain. Furthermore, since the R-T sample trajectories are nearly parallel to the wavefronts of the linear events, the apparent frequency of the events, in the R-T domain, is very low (ideally, DC). This makes the R-T transform ideal for analyzing and attenuating source-generated coherent noise (Henley, 2003). Attenuation can be accomplished directly by applying a low-cut filter to the traces of the R-T transform. Alternatively, the noise can be estimated by applying a low-pass filter in the R-T domain. The noise estimate can then be inverse-transformed back to the X-T domain, where it is subtracted from the original X-T gather. Although the methods are theoretically equivalent, in actual practice, we prefer the estimate-and-subtract approach, since it has less potential for lateral smear of the original data. Furthermore, we can enhance the subtraction process with a least-squares option.

The noises most suited to conventional radial trace attenuation are those which are generated directly by the source, and travel along the surface. The wavefronts of these noise events have a common origin at the source position and best fit the 'fan' pattern of the original R-T transform. It is desirable to be able to attenuate other linear events, as well, however, such as various refracted and waveguide modes, which tend to feature trains of parallel wavefronts with no common origin. Hence, we have included in our ProMAX radial trace filter module the capability of emulating a "dip" filter by the simple mechanism of using input parameters to create a "thin fan" transform with nearly parallel radial traces. Once the nominal dip velocity and the velocity 'range' for the thin fan are specified, the algorithm computes coordinates for a fictitious 'virtual' origin, and the

regular R-T transform uses these parameters to construct the sampling trajectories (Henley, 2003).

When coherent noise is aliased on a trace gather, due to too sparse spatial sampling during the data acquisition, there are a couple of 'tricks' that can be employed to improve noise attenuation, but the underlying reflection signal can be compromised by these techniques, if not carefully applied. In one technique, trace normalization can be applied in the R-T domain to reduce the amplitude disparity between noise wavefronts and background reflections; but this can disturb AVO relationships between amplitudes on neighbouring traces. In the other technique, linear moveout (LMO) can be removed from an input gather to reduce the noise aliasing for the purpose of estimating the noise with more fidelity; but the underlying reflections may then be aliased themselves and contribute an unwanted component to the noise estimate. The latter technique is explored more fully by Henley (2011).

PRINCIPLES OF R-T FILTERING

All techniques for attenuating noise with respect to seismic reflections use differences in the respective characteristics of the signal and noise to distinguish between them. In the X-T domain corresponding to conventional source or receiver trace gathers, the desired reflection events are characterized by hyperbolic trajectories in X-T space, and a particular frequency bandwidth that is usually deficient in energy below about 6 Hz. In this domain, so-called coherent noise is characterized by linear trajectories in X-T, and a broad range of frequencies, from well below the reflection band (ground roll) to well above (air blast). While frequency filtering in the X-T domain can attenuate some coherent noise, any part of the noise spectrum overlapping the seismic spectrum must remain untouched, or the reflection spectrum will be damaged. Likewise, linear noise can be attenuated, mostly on the basis of its apparent linear velocity, by an f-k filter; but such a filter will also attenuate any segments of reflections with the same apparent velocity and frequency content. Neither the X-T domain nor the f-k domain allow for total separation of reflection signal and coherent noise, and attenuation efforts in either domain often either fail to remove enough noise or damage the reflections, or both.

For much coherent noise, however, there is an additional discriminating characteristic that can be used—the apparent source position of the noise wavetrain on the trace gather. Even noise which has no obvious source point, like a refraction or waveguide mode, can be assigned a 'virtual source' point. Hence, each noise can be characterized not only by its apparent velocity, but by its apparent origin, as well. The radial trace transform is a mapping operation that gathers seismic amplitudes along linear trajectories in the X-T domain and interpolates them to single traces in the R-T domain. Since the sampling trajectories for the R-T transform are straight lines with a common origin, usually placed at the source point of the X-T gather, source-generated linear noises are mapped into compact groups of radial traces in the new domain while reflections remain spread laterally across the domain. Furthermore, because the sampling trajectories are nearly parallel to noise wavefronts, the apparent frequency of the noise is dramatically lowered. The R-T domain thus provides separation between signal and noise, not only in apparent velocity and origin, but in frequency as well. Figure 1 illustrates the process of transforming a trace gather from the X-T domain to the R-T domain.

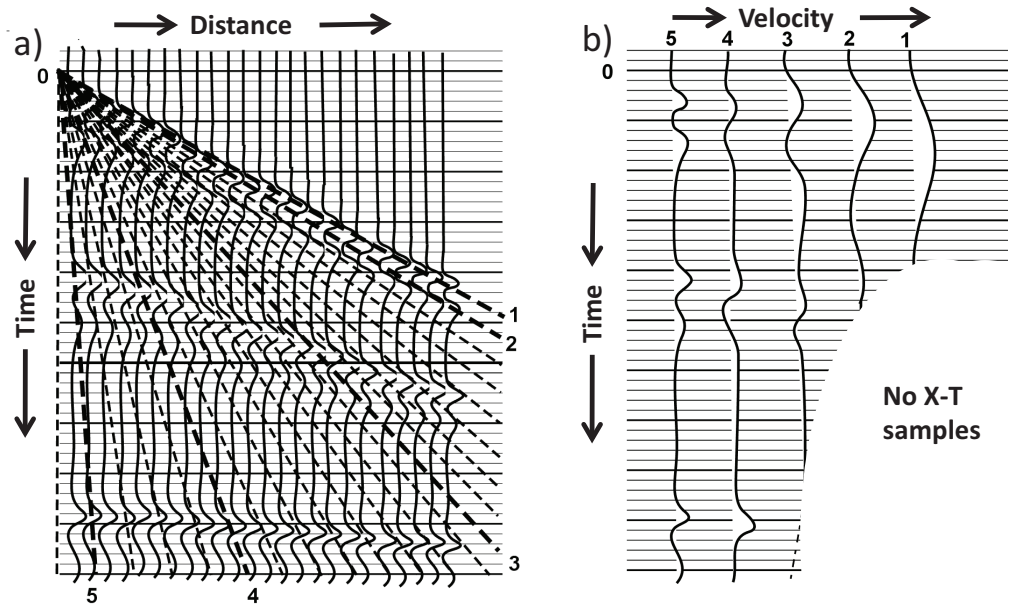

FIG. 1. Schematic showing how the radial trace (R-T) transform maps samples from linear trajectories in the X-T domain to vertical traces in the R-T domain. Representative numbered trajectories in the X-T diagram on the left correspond to numbered traces in the R-T diagram on the right. By convention, a radial trace is labelled with the apparent velocity of the trajectory used to map it.

Figure 2 shows a typical source gather containing both visible reflections and a moderate level of coherent noise. A radial trace transform of this gather appears in Figure 3, where it can be seen that direct arrivals and repeated initials transform into groups of low-frequency traces at the edges of the R-T gather, and ground roll becomes low-frequency traces near the centre of the gather.

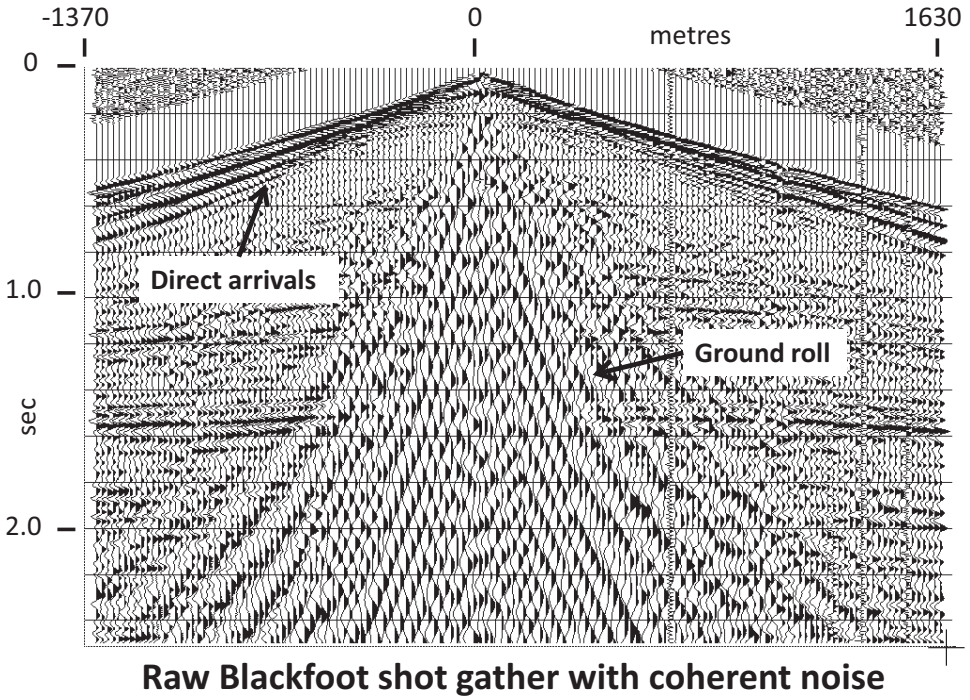

FIG. 2. Example of a shot gather with a moderate level of several types of source-generated coherent noise.

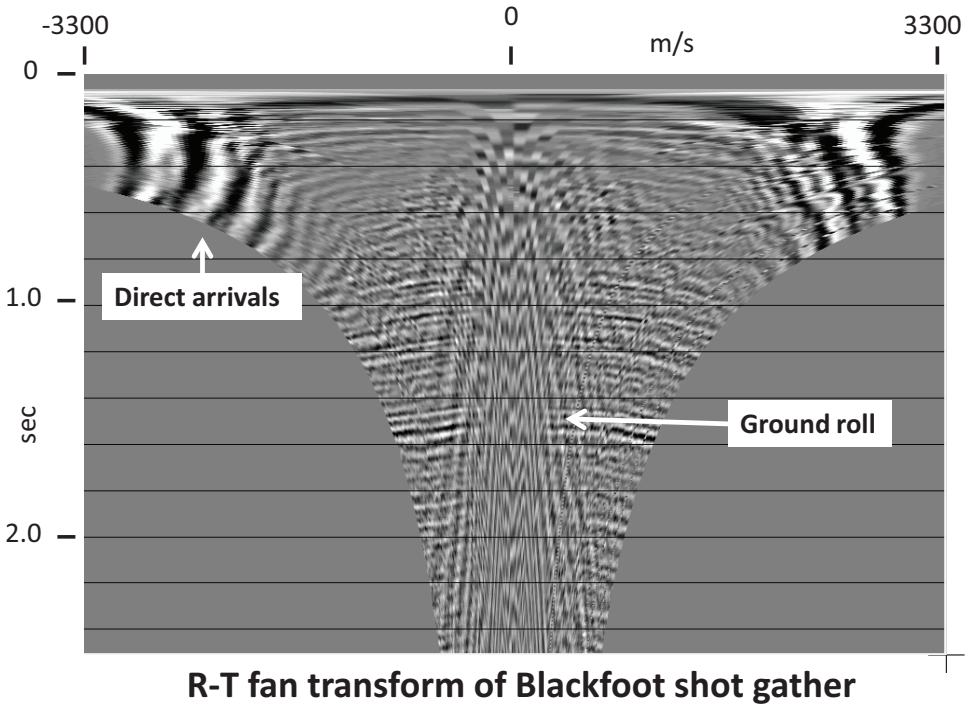

FIG. 3. R-T transform of the shot gather in Figure 2. Coherent noises become nearly vertical and much lower in frequency.

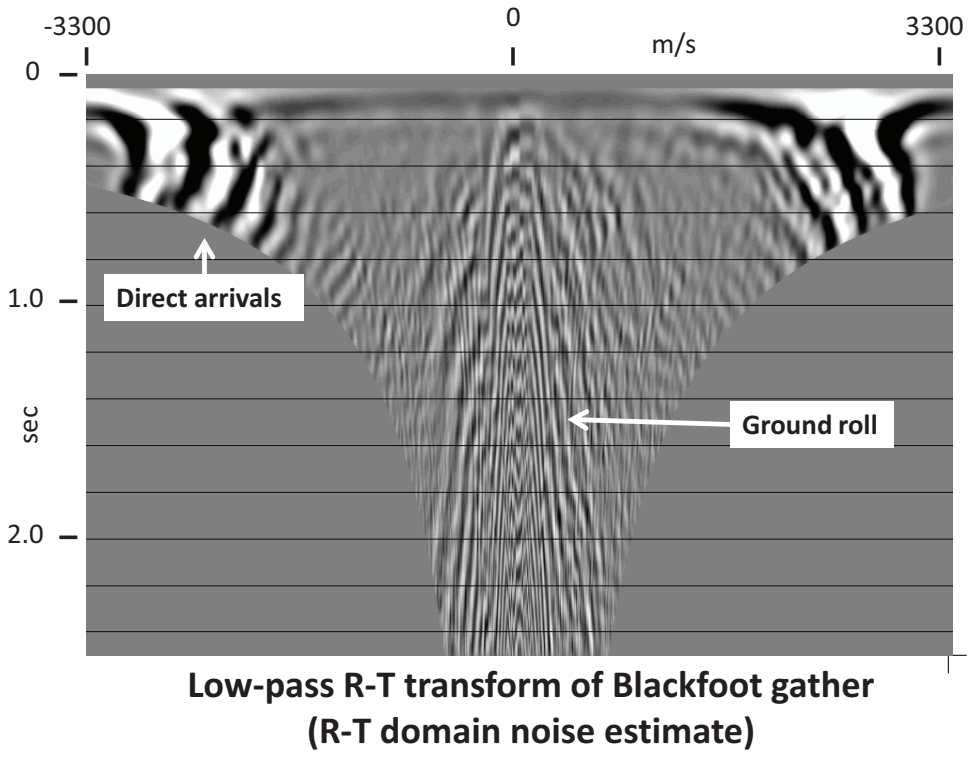

FIG. 4. Low-pass filtered version of the R-T transform in Figure 3. Reflections are no longer present.

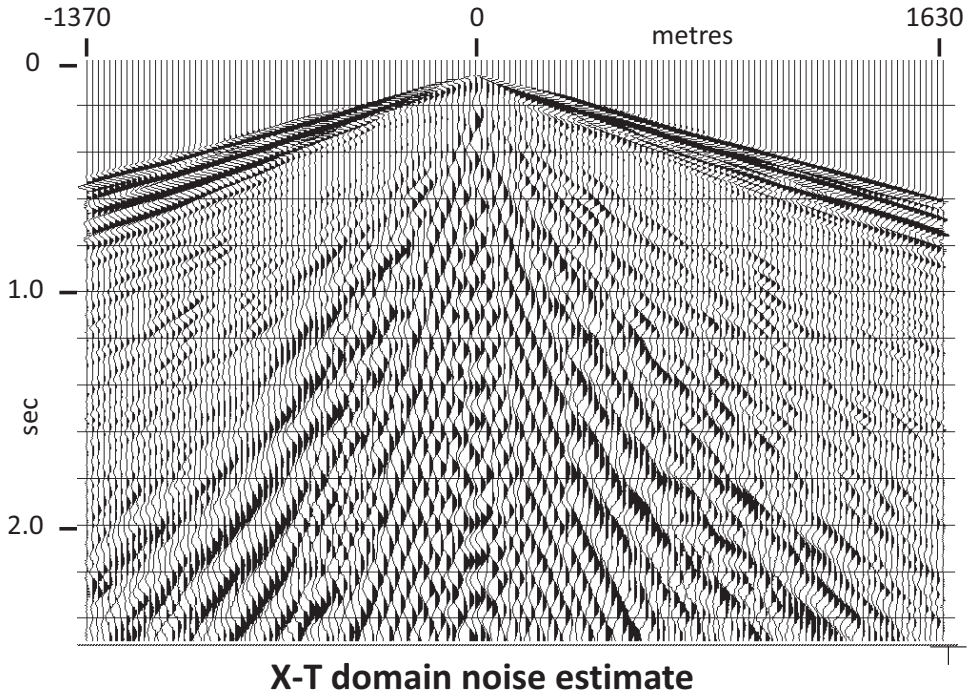

FIG. 5. Inverse R-T transform of the low-pass filtered R-T transform in Figure 4. This is the coherent noise estimate for the shot gather in Figure 2.

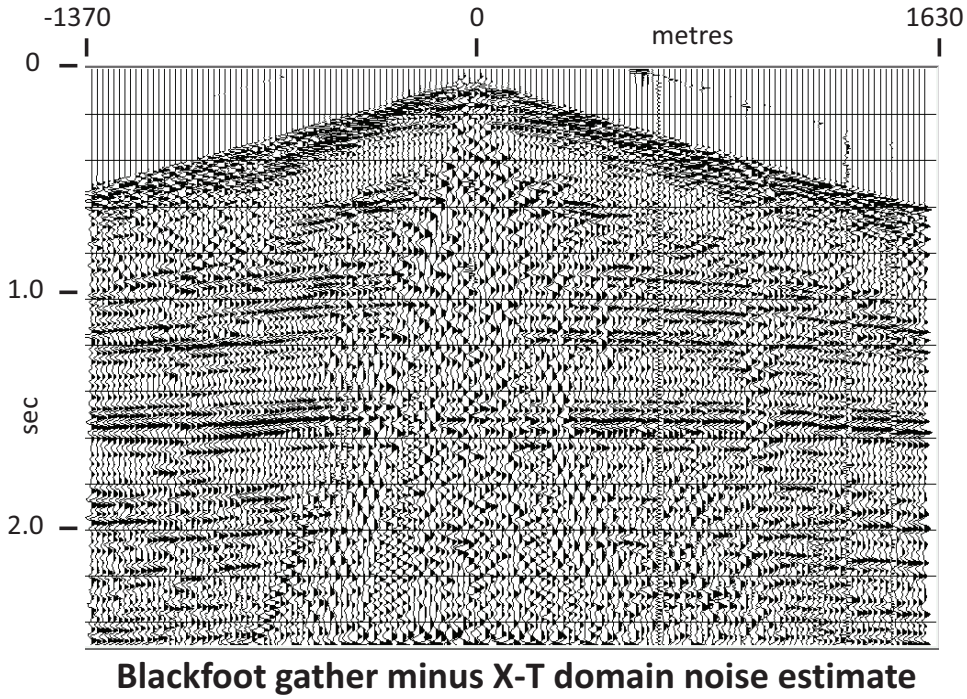

FIG. 6. Shot gather from Figure 2 after subtraction of noise estimate in Figure 5.

To illustrate the considerable frequency separation of the noise from signal, Figure 4 shows a low-pass version of Figure 3, and it can be seen that, while the coherent noise retains its full amplitude, almost no reflection energy appears. The inverse R-T transform of Figure 4 appears in Figure 5, our estimate of the source-generated noise in the original source gather, Figure 2. If we subtract this estimate from the original gather (properly scaled), we get the result in Figure 6. This sequence of figures thus demonstrates our main method for coherent noise attenuation in the radial trace domain. Note that the R-T method does not require knowledge of the type of noise—it targets all source-generated noise, regardless of its mode or velocity.

R-T FILTERING IN ACTUAL PRACTICE

The most effective application of R-T filtering is based on a combination of visual analysis of seismic trace gathers and trial application of R-T filter passes. The technique that we have developed over a number of years is an iterative one in which we first examine the raw data, apply a general purpose R-T fan filter to attenuate all overtly source-generated noise, examine the results for residual coherent noise, design dip filters to attack specific components of the residual noise, examine the results, and so on. Typically, we find that three or more passes of paired R-T dip filters, in addition to the initial R-T fan filter, will more than adequately attenuate most of the linear noise on a shot or receiver gather. Since all filter passes merely estimate noise and subtract it, the multiple passes do not smear reflections laterally like many f-k filters. Several years ago, we implemented a ProMAX module for applying radial trace filtering, either in the conventional ‘fan filter’ mode, or in the ‘dip filter’ or ‘thin fan’ mode. We demonstrate below the actual use of the module by presenting ProMAX processing flows and menu parameters.

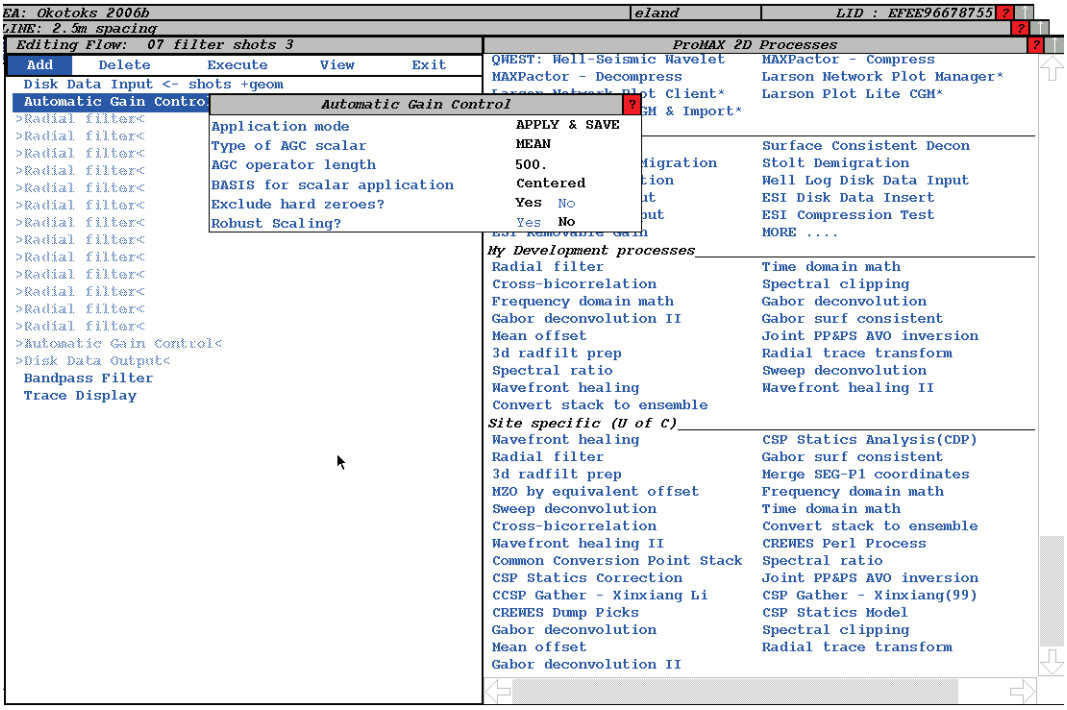

Diagnostic and design process flow for radial trace filtering (1)

FIG. 7. Processing flow for diagnosing coherent noise and designing filters to remove it.

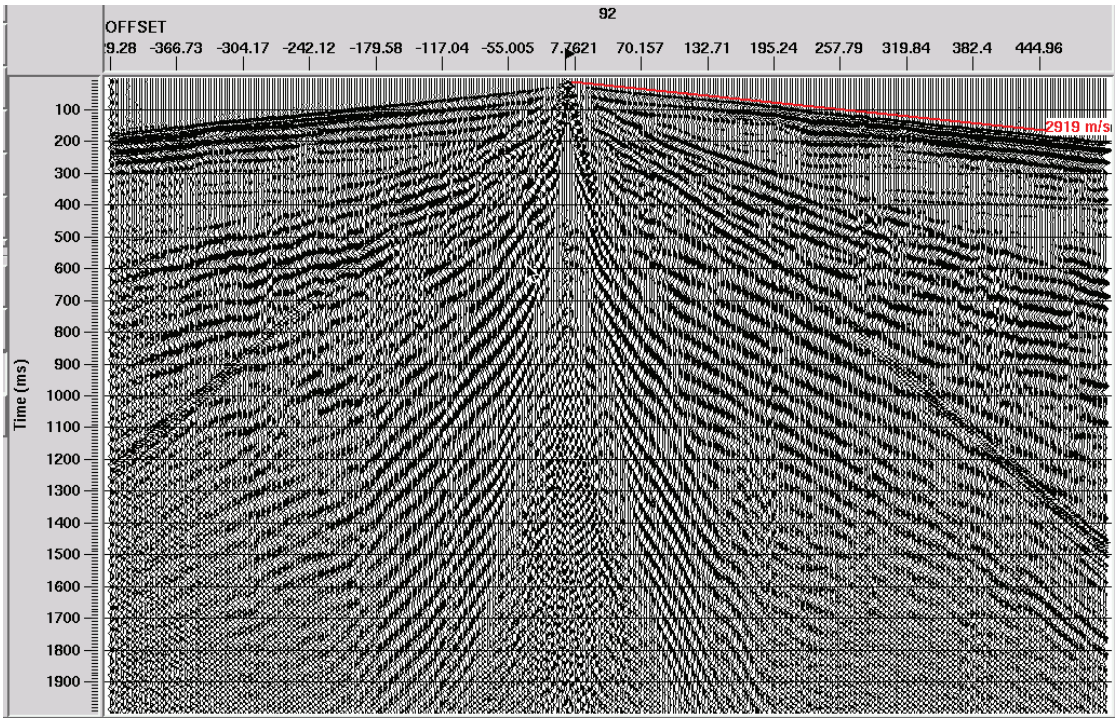

High resolution source gather with velocity of direct arrivals indicated

FIG. 8. Source gather display used to determine velocity for R-T transform aperture.

1. The first step in applying radial filter noise attenuation is to examine some typical trace gathers. Figure 7 shows a ProMAX test process flow which includes several passes of the radial filter algorithm (not activated for the initial execution). The Disk Data Input process reads in source gathers (preferred) or receiver gathers, sorted by ascending offset. These are often selected at intervals along a line, for testing purposes. As can be seen in the parameter window, the AGC process is used in 'apply and save' mode, so the AGC can be undone after noise attenuation. The reason for its application in the first place is to 'condition' the trace gather by reducing the magnitude disparity between amplitudes near zero time and offset and amplitudes near maximum time and offset. The bandpass filter process is applied to remove the visual distraction of any high frequency noise on the raw trace display. An example of a raw trace gather display from this flow is shown in Figure 8. This figure also contains a red line segment, created with the velocity tool in the trace display process, aligned with the first arrivals on the gather. The sole purpose of this line is to estimate the minimum and maximum velocities required for the first trial application of the radial filter process. The minimum and maximum are usually equal in magnitude and opposite in sign (linear velocities whose trajectories dip down to the left are negative, those which dip down to the right are positive).

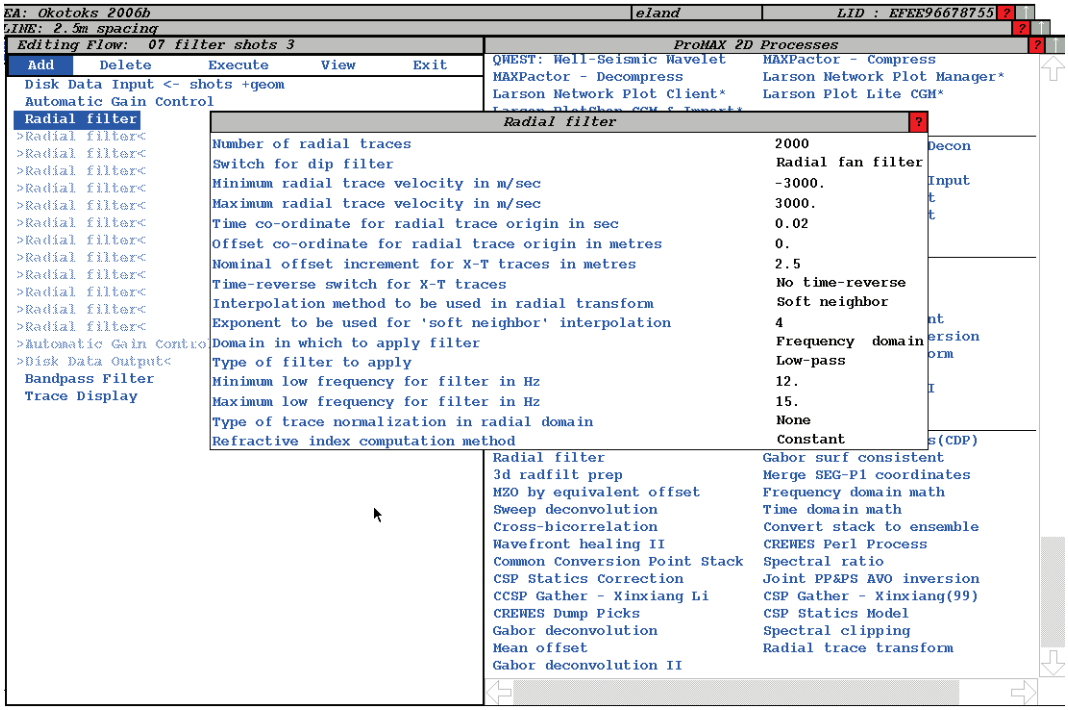

Diagnostic and design process flow for radial trace filtering (2)

FIG. 9. Processing flow for producing estimate and display of source-generated noise.

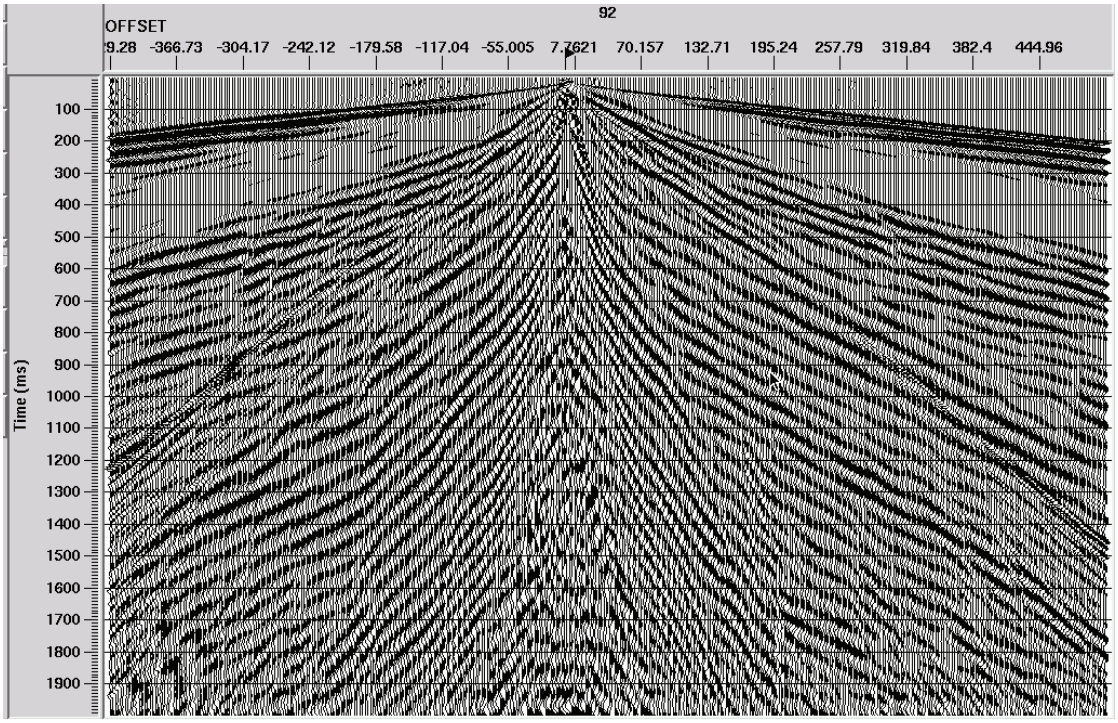

FIG. 10. The noise estimate created by the process flow in Figure 9.

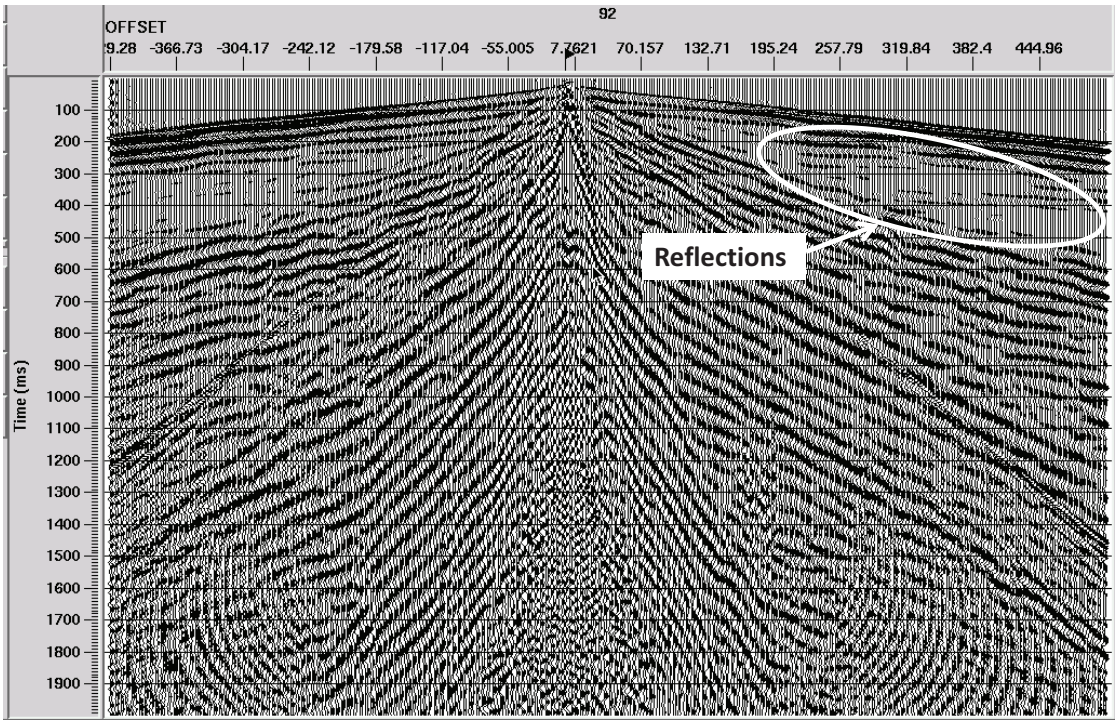

FIG. 11. A noise estimate where the low-pass filter parameters were too high, and some of the reflection signal was thereby included.

2. Next, we apply an analytic radial filter pass, in which we attempt to determine appropriate bandlimits for the actual filter application. The process flow is shown in Figure 9, with the menu window for the radial filter process. Note that the number of radial traces chosen is much higher than the number of input X-T traces per gather. This is necessary to avoid aliasing in the R-T transform, whose samples are distributed non-uniformly with respect to the original X-T domain. While the default value of 2000 is normally adequate, a larger number, like 4000 or even 6000 may be needed if the input trace gathers contain more than 500 traces or extend to more than 2 or 3 seconds in travel time. The minimum and maximum radial trace velocities are chosen to be slightly greater in magnitude than the velocity measured in Figure 8 in order to include the entire trace gather in the R-T transform and to exclude most of the trace samples above the direct arrivals. These velocities are the 'aperture' parameters for the R-T transform. The next two parameters can often be defaulted to zero, since they are the coordinates of the source relative to the origin of the trace display. In our example, the time coordinate is non-zero, since there is a small time delay between the display origin and the source initiation origin. The 'nominal offset increment' should be set to the average spatial distance between input traces, in this case, 2.5m. The next 4 parameters can always be defaulted. The 'type of filter to apply' offers five choices; for the initial diagnostic run, we choose low-pass, since this will then generate the noise estimate. The two frequency parameters which appear are the 'full-off' and 'full on' frequencies for a low pass filter. An initial guess for these two parameters should straddle the nominal low-frequency cutoff frequency of the raw seismic data (the -6 dB point, for example). For most conventional seismic data 6 Hz and 10 Hz are a reasonable starting point. For the high-resolution data shown here, 12 and 15 Hz were chosen initially. The last two parameters in the menu are always defaulted. Figure 10 shows the result of running the flow in Figure 9 with low-pass filter values which exclude virtually all the useful seismic reflection band, since only noise can be seen on the display. Figure 11, however, shows the result when these frequency values are too high and include some of the reflection band. Weak reflection energy can be seen on this gather (elipse). A few tests with different pairs of frequency values should enable the user to find values which are as close as possible to the low frequency cutoff of the reflections without including reflection energy. The lower value should typically be no more than 75 percent of the upper value in order to avoid creating artefacts due to sharp filter rolloff. Values chosen during this diagnostic step are safe to use for all subsequent filter passes, although lower values can be chosen for dip filters whose apparent velocity is relatively low.

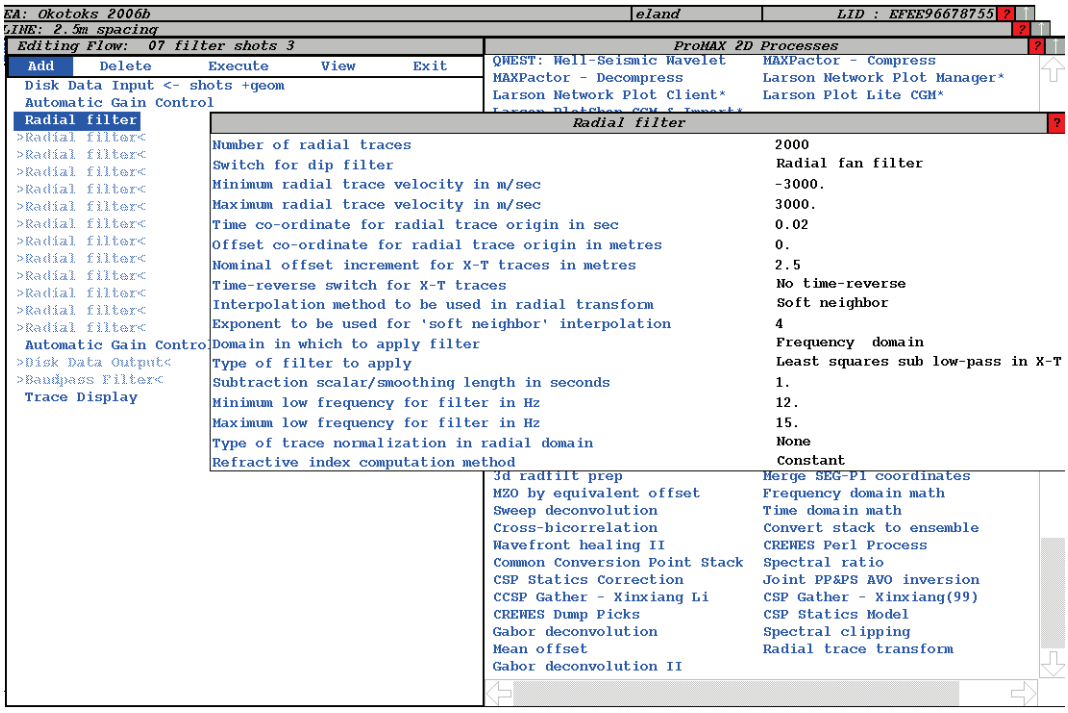

Diagnostic and design process flow for radial trace filtering (3)

FIG. 12. The process flow for applying the first R-T domain filter (subtracting the estimate in Figure 10 from the raw shot in Figure 8).

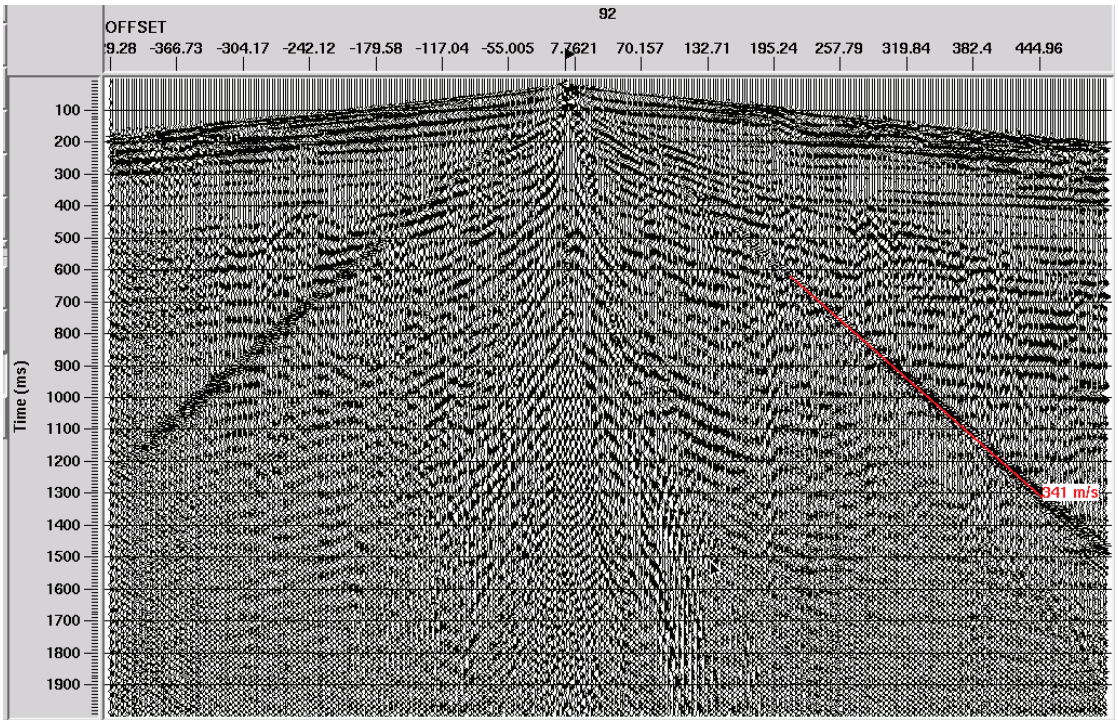

Source gather after radial fan filter application. Velocity of airborne noise estimated.

FIG. 13. First pass of R-T filtering applied, velocity for airborne noise estimated.

3. The next trial run is done with the Flow shown in Figure 12, in which the same filter pass as in step 2 is used, except that for this execution, the 'type of filter to apply' is chosen to be 'subtract low-pass in X-T' or 'Least squares sub low-pass in X-T'. With the first choice, the subsequent parameter is a scalar to apply to the noise estimate before subtraction (best defaulted to 1.0); while with the second option, this parameter is the length in seconds of the smoothing parameter for the least-squares subtraction algorithm (default of 1.0 is still a good choice, but anything up to the total trace length can be used). Least-squares subtraction can be slightly more effective for noise attenuation, but can extend execution time. Figure 13 shows our initial trace gather (Figure 8) after application of this subtraction filter. Also shown in this figure is a velocity trajectory aligned with one of the prominent linear noises surviving the first estimation and subtraction (airborne noise). Its velocity is used in the creation of a pair of trial radial trace dip filters for the next step.

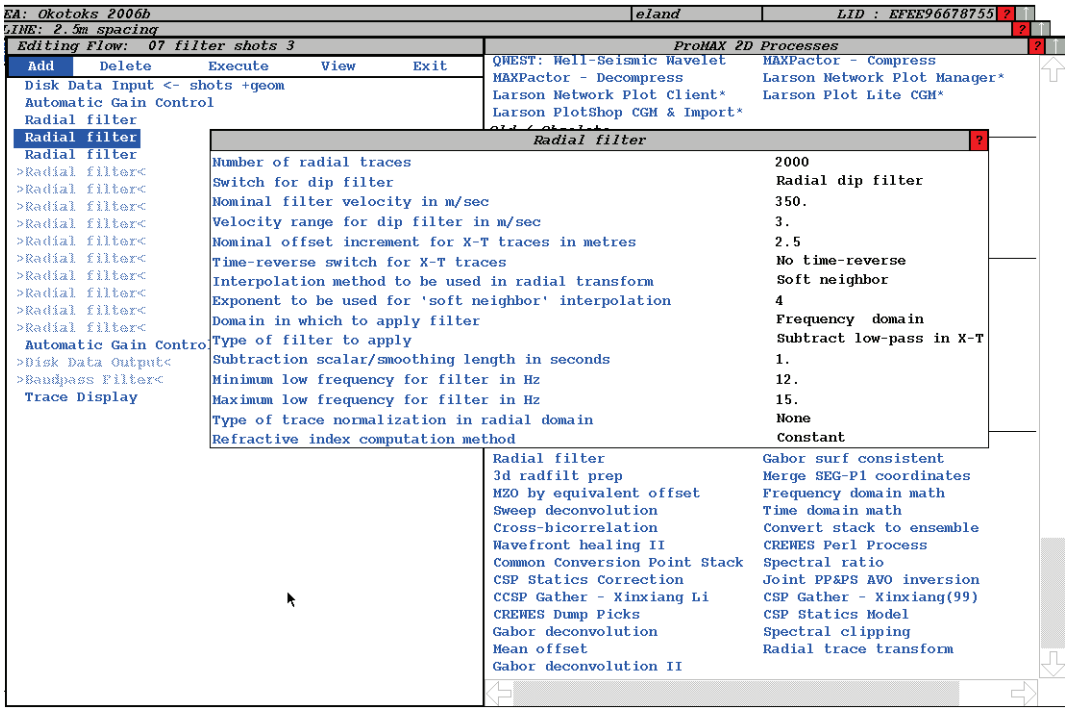

Diagnostic and design process flow for radial trace filtering (4)

FIG. 14. Processing flow for one pass of R-T fan filtering and a pair of R-T dip filters designed to attenuate airborne noise.

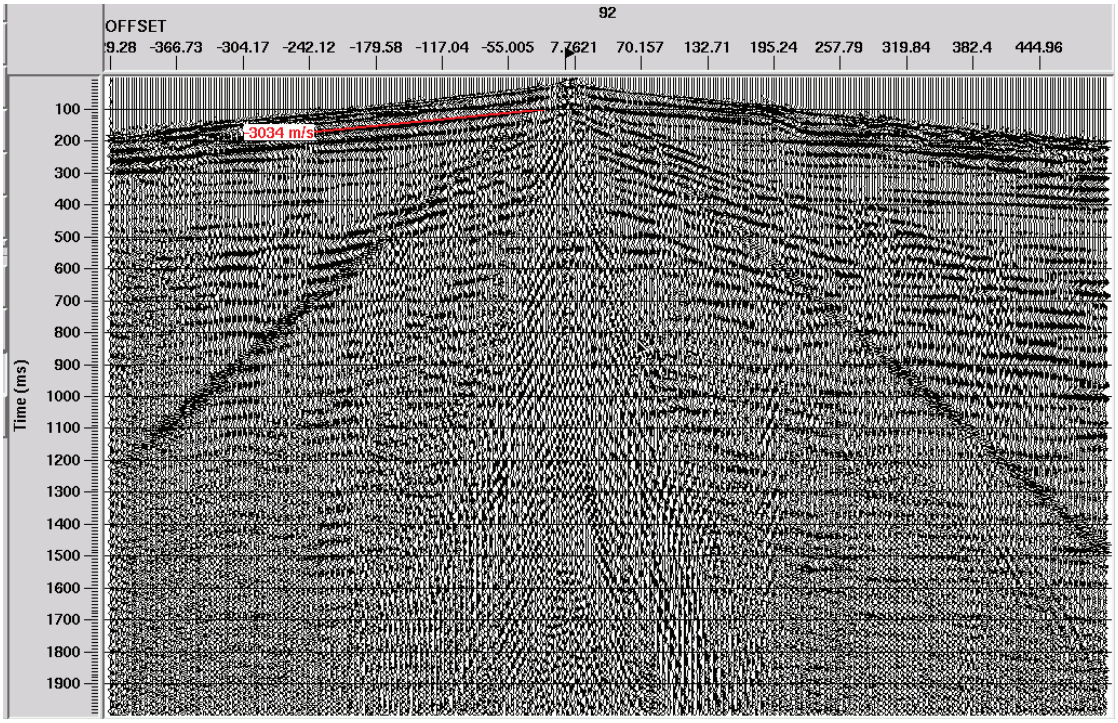

Source gather after radial fan filter, two dip filters. Velocity of near surface event shown.

FIG. 15. One pass of R-T fan filtering plus R-T dip filters for airborne noise. Velocity for linear event near surface estimated for next dip filter pass.

4. Figure 14 is the process flow as it appears after inserting the two radial dip filters. We show the menu for only one of the filters; the other is exactly the same except for the opposite sign on the 'nominal filter velocity'. Note that the second parameter in the radial filter module is now selected as 'radial dip filter' rather than 'radial fan filter'. In this mode, the radial filter algorithm creates a 'thin fan' of radial traces whose 'nominal' apparent velocity is the next parameter. The fourth parameter is the velocity range, or 'width' in velocity of the thin fan of traces. For a small width, the radial traces created are very nearly parallel over the entire trace gather, while for a larger width, the traces sampling the top of the gather will have significantly larger apparent velocity than those sampling the bottom of the gather. Normally, this parameter would be set to 1% to 10% of the nominal velocity. The rest of the parameter choices for a radial dip filter are the same as for a fan filter. Figure 15 shows the result of applying the pair of radial dip filters in the flow in Figure 14 to the output of the fan-filter. Also displayed is another straight line segment aligned with a prominent residual linear noise of a particular velocity, which can be used in the creation of another pair of radial trace dip filters. Often, when energy of a specific relatively high velocity is estimated and subtracted, the most visible residual coherent energy has an apparent velocity about half that attenuated in the previous filtering step, obviously an alias of the earlier energy.

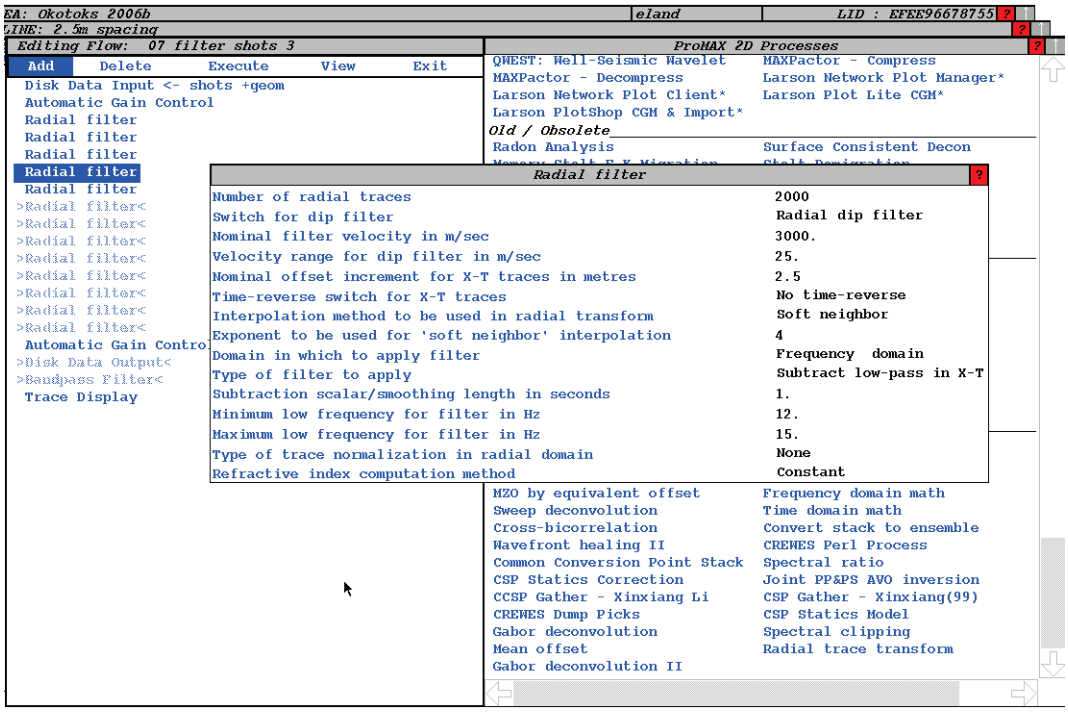

Diagnostic and design process flow for radial trace filtering (5)

FIG. 16. Processing flow showing the next pair of dip filters to attenuate the high-velocity noise in Figure 15.

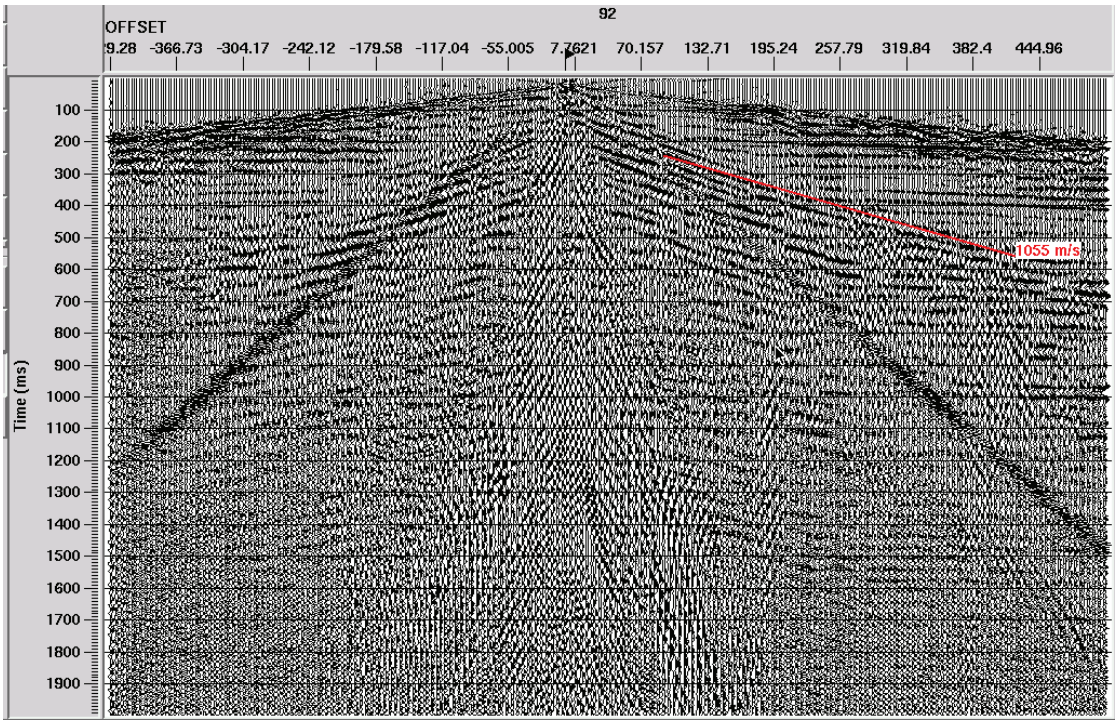

Source gather after radial fan filter, two sets of radial dip filters, velocity for next event.

FIG. 17. R-T fan filter applied, R-T dip filters for airborne noise applied, R-T dip filters for high velocity noise applied, next noise velocity estimated.

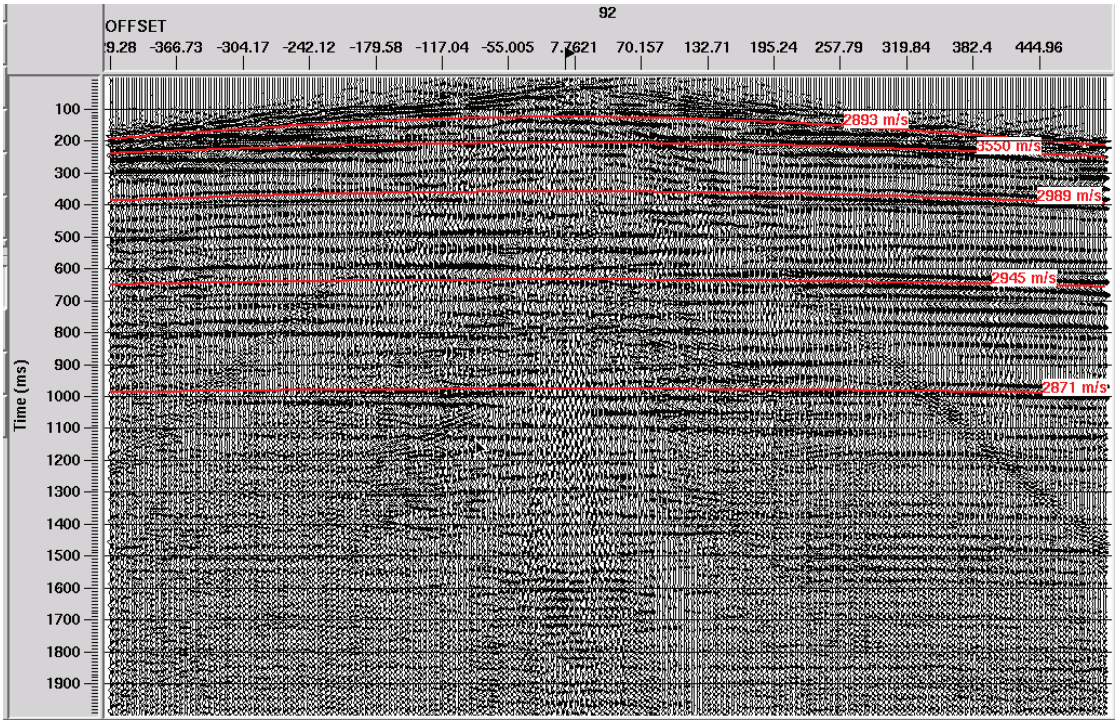

FIG. 18. Shot gather from Figure 8 after application of all R-T filters (one R-T fan filter, 6 pairs of R-T dip filters). Underlying reflections are now visible and some have been identified by fitting hyperbolic velocity curves.

5. The process flow including the new pair of dip filters is shown in Figure 16, as is the menu window with the parameters for one of the new filters. Figure 17 shows the result of applying these filters after those in Figure 15. As can be seen, the process of analyzing dipping noise trains and removing them with pairs of dip filters can be continued for several steps. With each filter application, the underlying reflections should become more prominent. At some point, however, even though our filtering consists of modeling each noise and subtracting it, the underlying reflections can suffer some degradation. One of the purposes of the step-by-step testing of additional stages of filtering is to determine the point at which the filtering no longer improves the visibility of reflections, or begins to degrade them. Figure 18 shows the trace gather from Figure 8 after all the significant radial filter passes have been applied. On this display, the velocity tool in the ProMAX trace display operation has been used to align several hyperbolae with prominent reflections, to show the events once obscured by coherent noise (Figure 8).

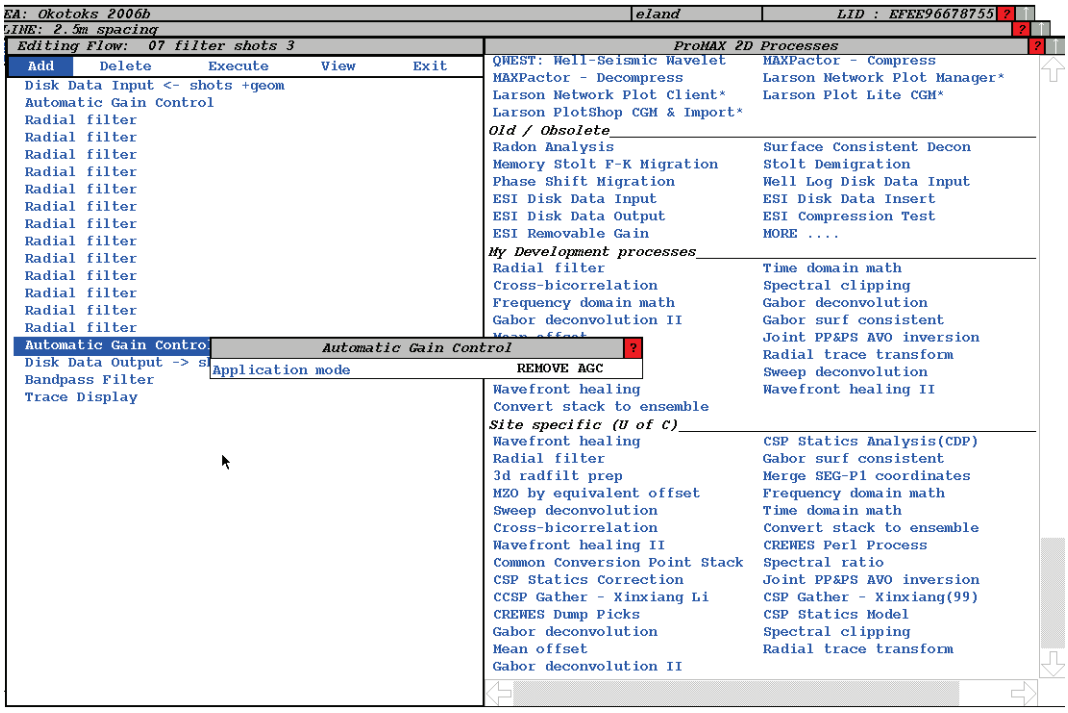

Diagnostic and design process flow for radial trace filtering (6)

FIG. 19. Complete processing flow for applying all R-T domain filters, removing AGC, and writing filtered shots to an output file. It can be useful to monitor the run by leaving the bandpass and trace display operations active.

Once a filter sequence has been designed for application to the trace gathers, the process flow is modified as shown in Figure 19, to include another AGC operation in which the AGC is removed to restore proper reflection amplitudes. This is necessary in order for subsequent application of non-stationary deconvolution to work properly. This flow also shows a 'Disk data output' process for saving the filtered shots to a new file. It is often useful to retain the bandpass filter and trace display operations in this process flow, so that the filtering process can be monitored on each gather, if desired.

OTHER R-T FILTER SCHEMES

In addition to the estimation and subtraction of filters modeled in the R-T domain, the 'normal' mode of coherent noise attenuation, there are other operations that can be used to attenuate specific instances of coherent noise. One such operation is available within the radial filter module itself, while others require use of the separate 'radial trace transform' module in both forward and inverse modes. We illustrate one example of each.

Normalization in the R-T domain

Figure 20 shows an example of a shot gather generated in the CREWES physical modeling facility (Wong, et al, 2007, 2008, 2009). As can be seen, the relatively weak reflections are almost completely dominated by the very strong surface wave and its time-delayed repeat, and can't even be seen properly unless the trace amplitudes are boosted high enough to severely clip the linear arrivals. While this energy can be

attenuated in the regular radial filter process, a simpler way is to equalize trace amplitudes in the R-T domain.

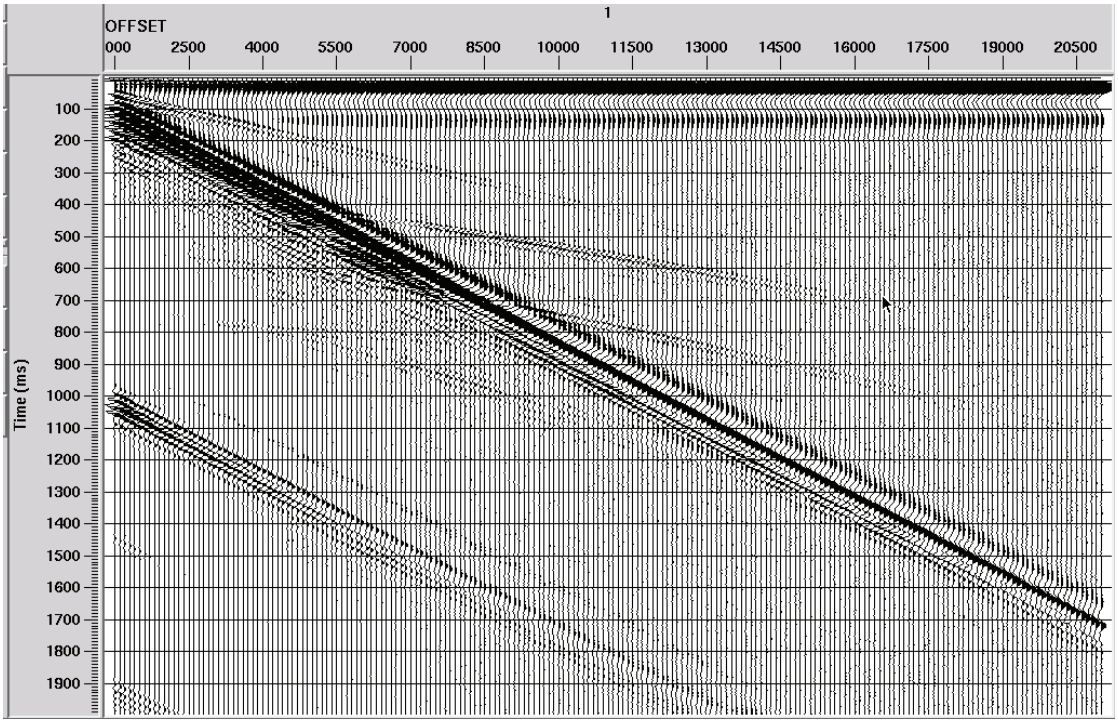

FIG. 20. Shot gather created by the CREWES physical modeling facility. Linear noise totally dominates the shot record, leaving reflections barely visible.

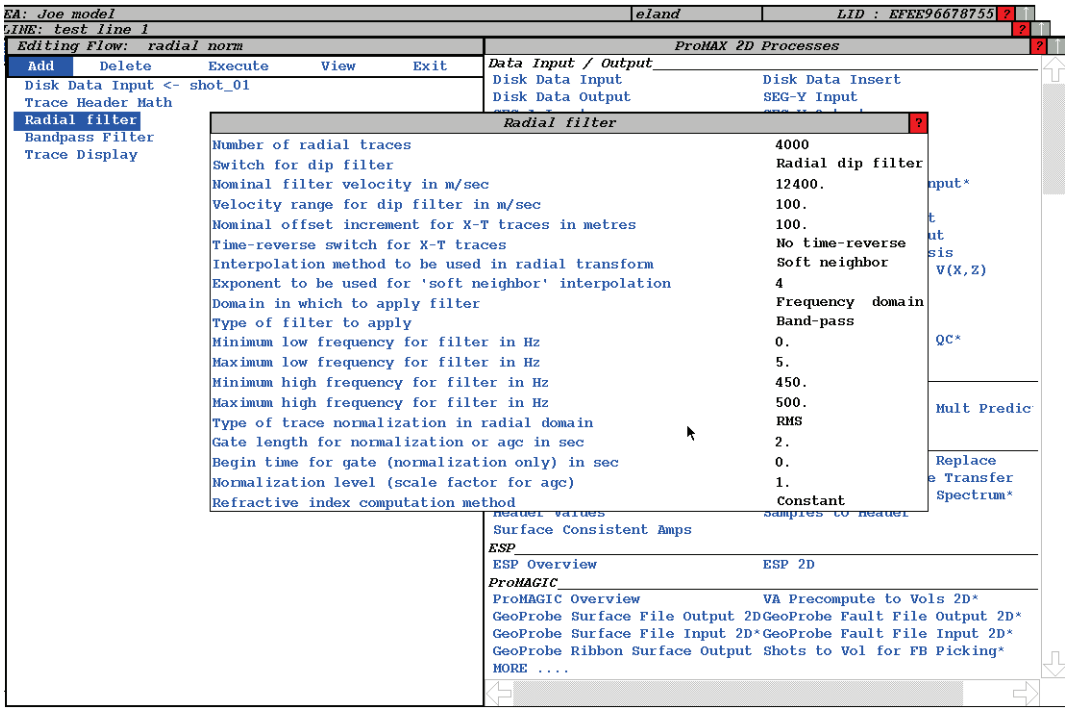

Process flow for radial trace normalization

FIG. 21. Process flow for amplitude normalization in the R-T domain.

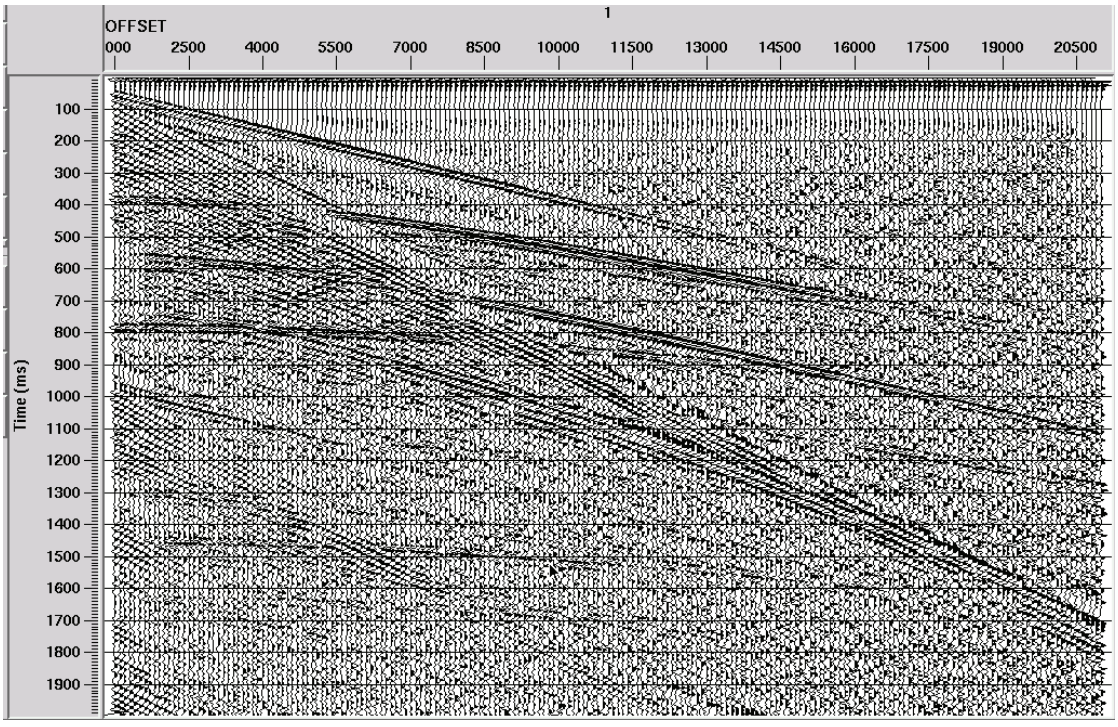

Linear noise trains attenuated with respect to reflections by AGC in the R-T domain

FIG. 22. Result of applying short-window AGC in the R-T domain...no filtering applied.

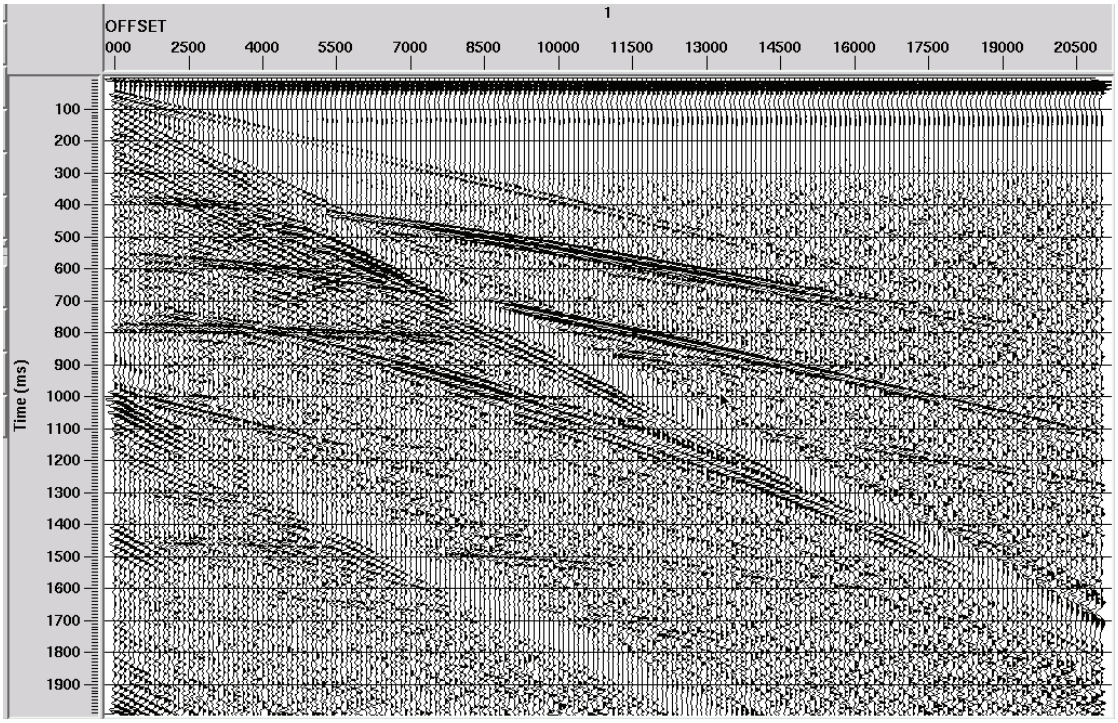

FIG. 23. Result of applying whole trace normalization in the R-T domain...no filtering applied.

Figure 21 shows a process flow and the menu window for this operation, using the radial filter module. The idea is to create an R-T filter whose trajectories are parallel to the wavefront of the strong noise, in this case, a radial trace dip filter with the same apparent velocity as that of the noise wavefront. Instead of applying a filter to attenuate some portion of the frequency band of the R-T domain, however, we choose 'bandpass' for the 'type of filter to apply' then select frequency parameters for the filter which more than encompass the seismic band, so that all events are passed with no attenuation. However, instead of 'none' for the 'type of trace normalization in radial domain' we choose either 'abs', 'rms', or 'agc'. In the case of 'abs' or 'rms' the subsequent parameter should be set to the trace length of the X-T traces; but if 'agc' is chosen, a much shorter length, like 0.1 sec, can be chosen. Whichever method is chosen, the effect is for radial traces containing samples just ahead of the noise wavefronts to be scaled up to match the amplitudes of radial traces containing samples within the noise waveforms, thus suppressing the noise waveforms with respect to background amplitudes. The 'agc' method is the most effective, as can be seen in Figure 22, but applying the agc operator in the R-T domain effectively applies it across multiple traces in the X-T domain, thus altering AVO relationships. The effects of the 'abs' or 'rms' options are less profound, but they're somewhat less effective, leaving lateral shadow zones within the noise trains, as can be seen in Figure 23.

Spectral editing in the R-T domain

Some coherent source-generated noises are so difficult to attenuate that they require special measures. One of these is the notorious ice flexural wave often recorded on

floating ice in the Arctic (Henley, 2004). Figure 24 shows an example of this noise, which is so strong that it renders any reflections invisible. One of its obvious characteristics is its large dispersion; and that is also the basis upon which it can be attacked. The dispersion means that each discrete frequency component of the noise essentially travels at a different velocity. Hence, the traces of an R-T fan transform each capture a different, discrete frequency component of the noise. Because the noise is so powerful, these discrete noise frequency components are much stronger than the background seismic spectrum captured by each radial trace...they appear as spikes superimposed on the background seismic spectrum. They are thus vulnerable to spectral editing. Our 'spectral clipping' algorithm is designed to look for these spectral spikes and to replace them by the median spectral values in the vicinity of the spikes (Henley, 2005). Figure 25 is an example process flow for applying spectral clipping in the R-T domain. Note that in this instance, we use the radial transform module instead of the radial filter module, because we need external access to the radial traces themselves. Note that the parameters required for the forward R-T fan transform are similar to those required for an R-T domain filter pass, except that there are no parameters pertaining to filtering. The output from the module as shown in Figure 25 is 2000 radial traces, each with a slightly different apparent velocity. Because of the large dispersion in the ice flexural wave, each radial trace captures a different specific frequency component of the noise. The spectrum in Figure 26 shows a spectrum of one of the radial traces; the spectral peaks due to the particular frequency component of the ice wave, and its harmonics, are clearly visible. Each of the 2000 radial traces will have a similar spectrum, except that the spikes will occur at different frequencies, depending upon the apparent velocity of the radial trace.

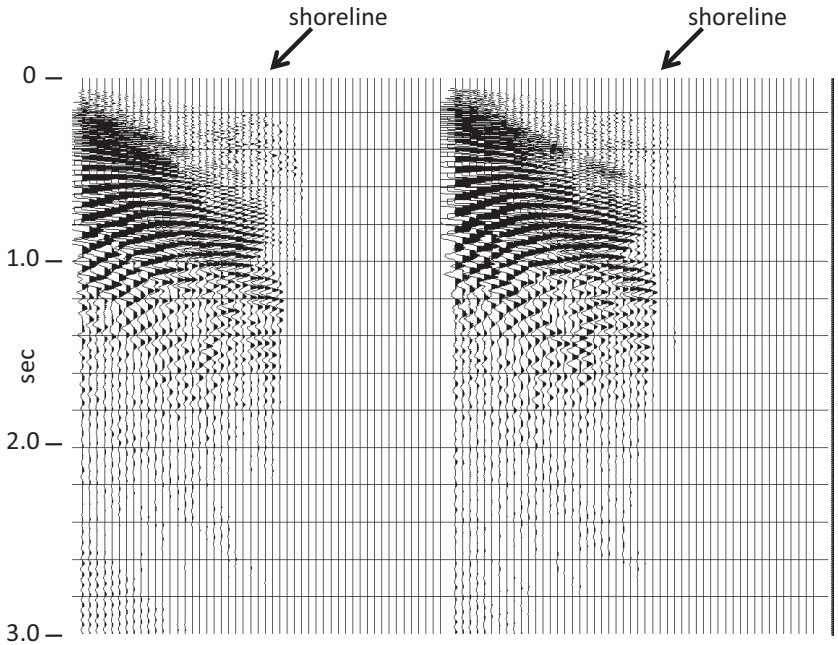

FIG. 24. An example of ice flexural wave noise on source gathers from the Arctic.

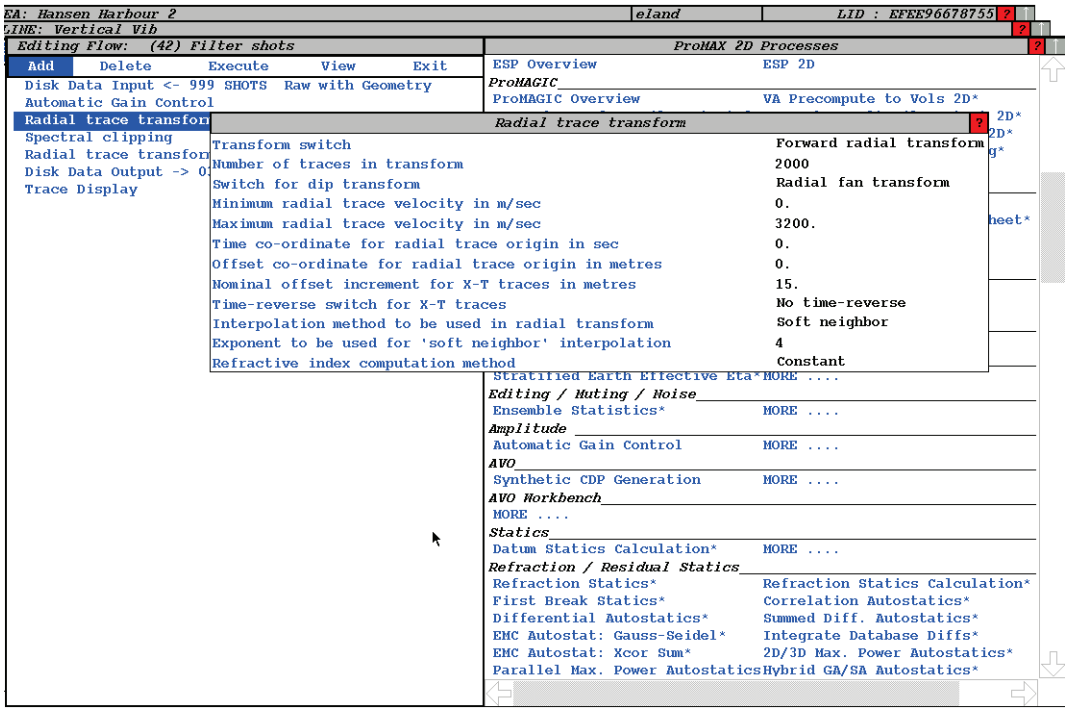

Process flow for spectral clipping in the radial trace domain (1)

FIG. 25. A processing flow for applying spectral clipping in the R-T domain to eliminate the sharp spectral peaks in R-T spectra caused by the ice flexural wave. R-T transform parameters shown.

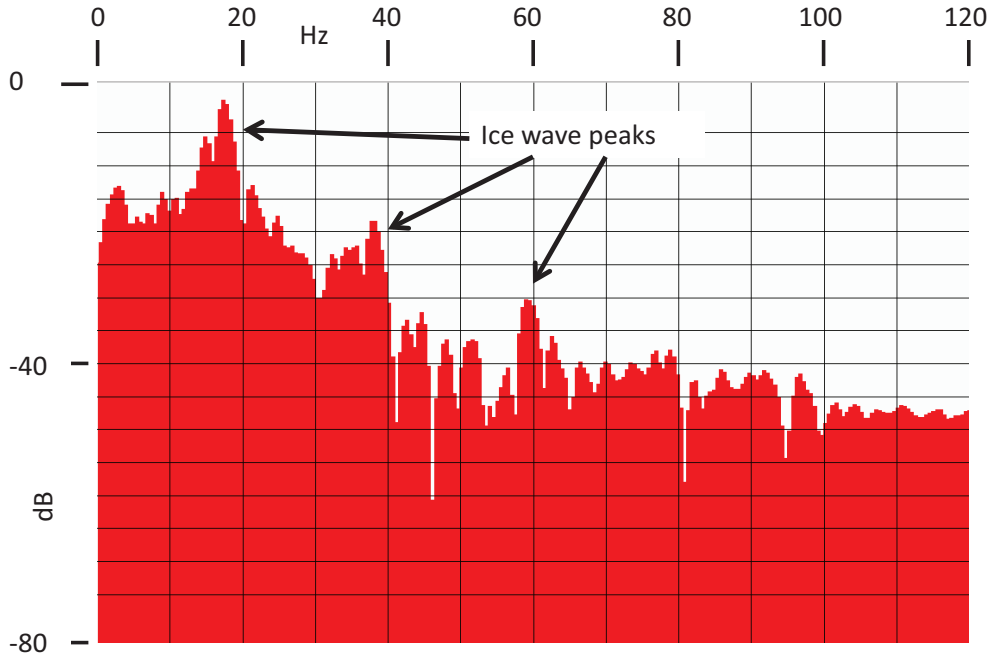

Spectrum of radial trace with ice wave noise

FIG. 26. Ice flexural wave superimposes tall, narrow peaks on background seismic spectrum of one of the R-T domain traces created from a shot gather in Figure 24.

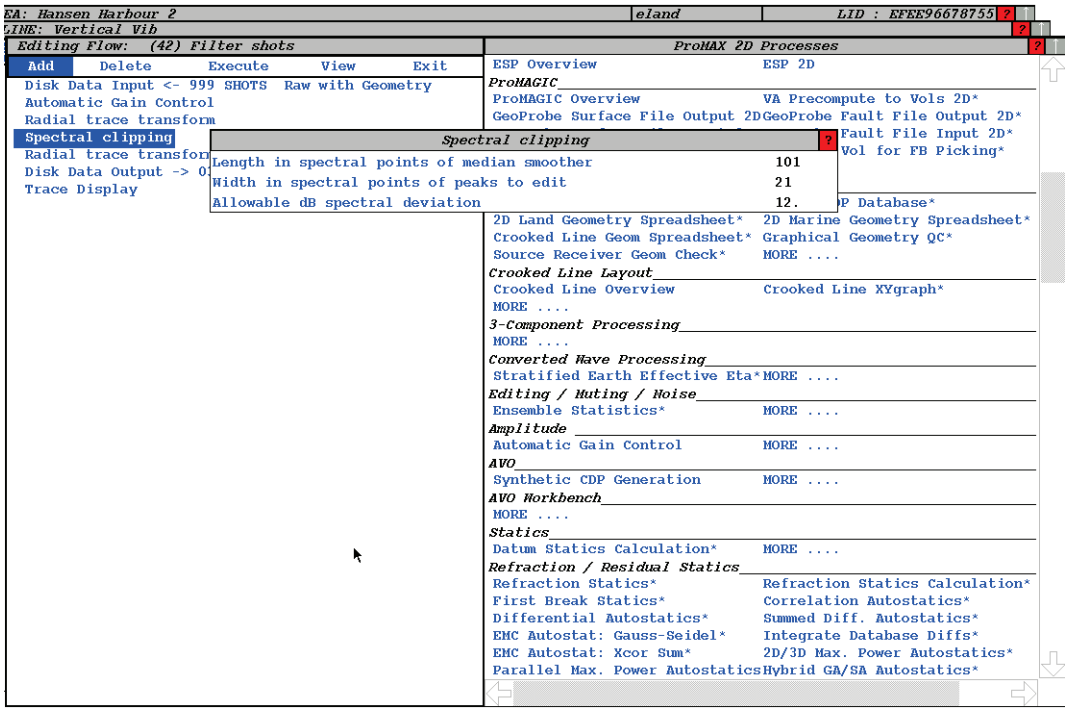

Process flow for spectral clipping in the radial trace domain (2)

FIG. 27. Processing flow for applying spectral clipping in the R-T domain. Spectral clipping parameters shown.

The next module in the ProMAX flow is 'spectral clipping', Figure 27, which does the automatic non-linear spectral editing required for eliminating the ice wave spikes. The three parameters may be safely defaulted in most cases. The length of the median smoother for the spectrum is very insensitive...the purpose of the smoother is just to provide a very smooth average spectrum, with no peaks or notches, against which to compare the actual spectrum. The next parameter, which is also very insensitive, simply chooses the number of spectral points in the vicinity of detected spikes or notches that will be set to the nominal median value. The one parameter which can significantly affect performance is the final one: the threshold against which all spectral values are compared. If any individual raw spectral amplitude differs by more than this threshold from the smooth median spectrum in its vicinity, that amplitude and its immediate neighbours are set to their corresponding median values. The default value of 12 dB works well for most data. A value as small as 6 dB can be used, but resulting spectra may have some of their legitimate peaks and valleys edited out, as well. Values larger than 12 dB can cause the algorithm to pass spikes and notches that should be edited. Figure 28 shows the same spectrum as Figure 26 after the spectral clipping operation. The spectra of all the radial traces are similarly edited by the spectral clipping operation.

The radial trace transform module which follows the spectral clipping in Figure 29 applies the inverse R-T fan transform. All the parameters should be set as shown. The presence of the 1 in the 'number of traces in the transform' triggers the inverse to reconstruct an X-T gather that is nearly the equivalent of the input gather, except that the offset values are exactly uniformly spaced. The 'method for offset computation' should

always be set to 'linear', since the alternative selections are special purpose applications, unrelated to the actual R-T inverse operation. The result of applying the process flow in Figures 25, 27, and 29 to the receiver gather in Figure 24 is shown in Figure 30. As can be seen, the ice flexural wave noise is greatly diminished, and fragments of reflections can now be seen.

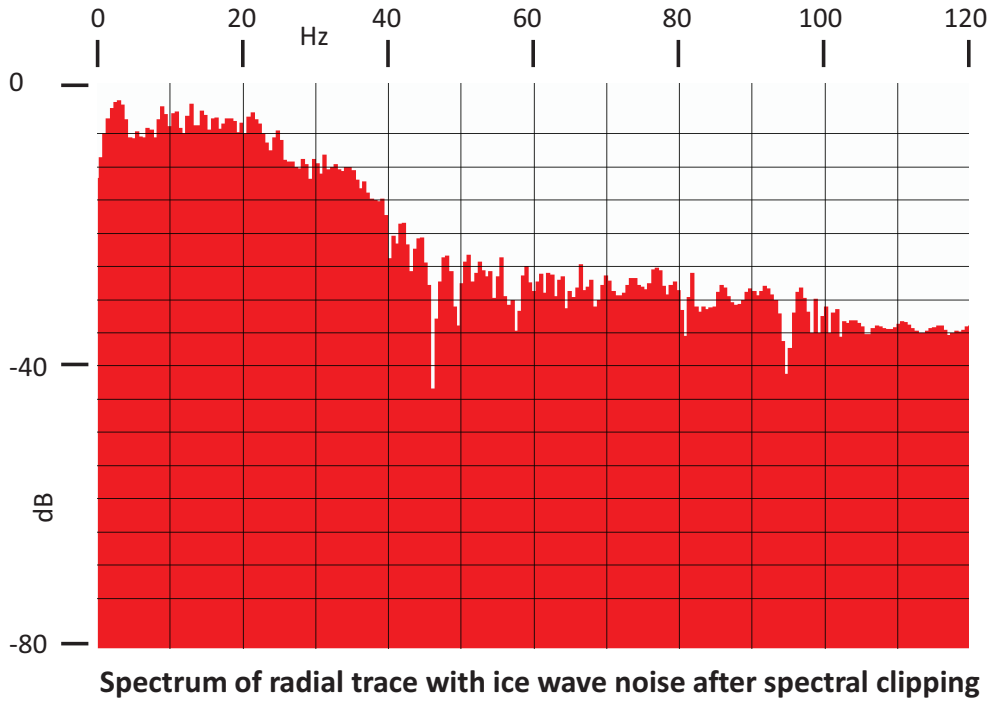

FIG. 28. Spectrum of R-T trace after the ice flexural wave spikes have been edited out by spectral clipping.

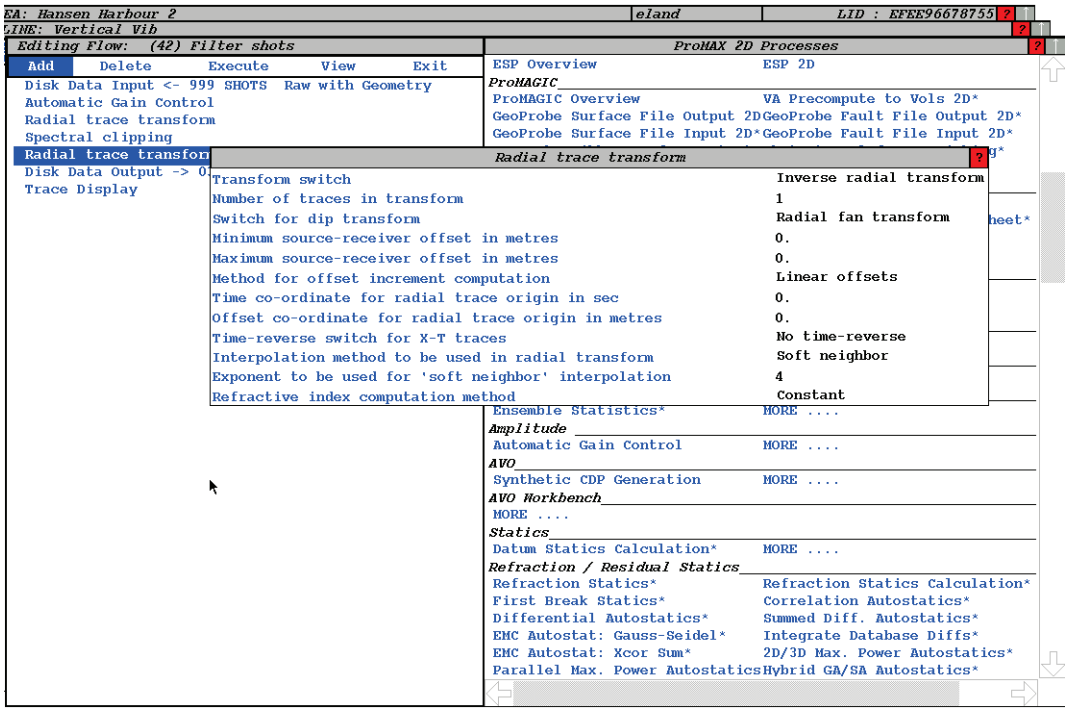

Process flow for spectral clipping in the radial trace domain (3)

FIG. 29. Processing flow for R-T domain spectral clipping. Inverse R-T parameters shown.

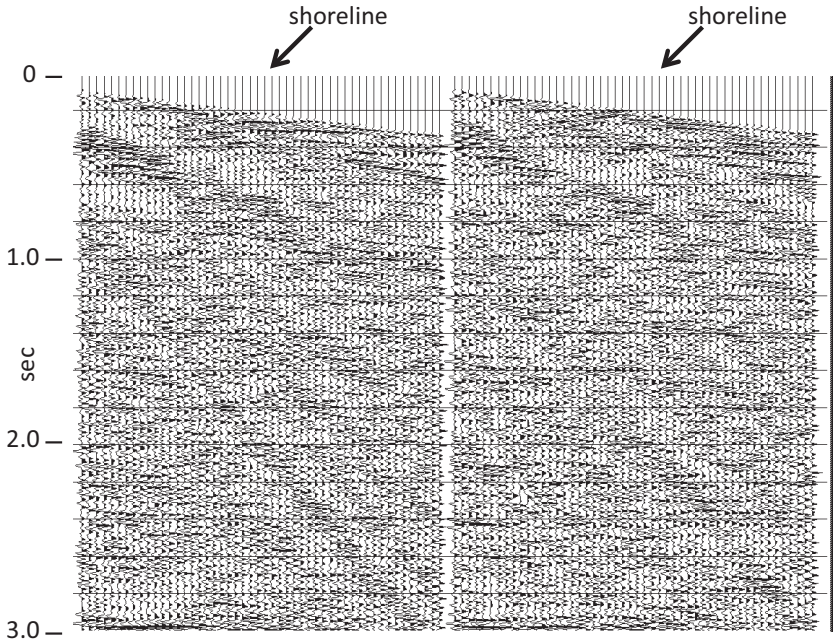

RT domain spectral clipping applied, followed by XT domain spectral whitening. Fragmentary reflections are visible

FIG. 30. Shot gathers from Figure 24 after R-T domain spectral clipping. Weak reflection fragments are now visible

SUMMARY

Although R-T-based techniques for attenuating coherent noise have been available for several years, this report is our first actual tutorial on using our ProMAX modules to apply the techniques to real seismic data. We have presented the 'standard' method, which involves a step by step analysis and design of a cascade of R-T domain filters, which estimate noise components and subtract them from the input data. Because of the 'hands-on' approach, an experienced processor can design and apply a filter process flow of great effectiveness for any particular data set. Our approach attempts to remove noise iteratively, rather than all at once, like a more conventional f-k filter approach. Since the R-T transform allows more discrimination between linear noise events and long-offset limbs of reflections with similar dips than does the f-k transform, a series of R-T filters can be designed which eliminates most coherent noise while leaving reflections largely intact. This is especially true for shallow reflections whose longer offsets are often obscured by linear first arrival events.

In addition to our 'standard' filter approach, we have shown how to apply two kinds of 'specialty' operations in the radial trace domain, as well. R-T amplitude normalization can be useful in reducing very energetic linear noises to levels comparable to the underlying reflections without altering the frequency content. If ordinary normalization is used in this process, AVO information in the underlying reflections survives, but if the more effective AGC is used, AVO relationships will be disturbed. The other specialty operation illustrated here is spectral clipping in the R-T domain, specifically aimed at very strong, highly dispersive noises like the ice flexural wave recorded on floating ice in the Arctic, or some instances of ground roll. The spectral clipping operation itself is non-linear, and it can be extremely effective on very strong noises, as long as they are sufficiently dispersive to resolve into narrow frequency bands in the R-T domain.

We hope that the specific ProMAX process flows and procedures described here will assist sponsors in application of R-T domain techniques for the effective attenuation of coherent noise on seismic data.

ACKNOWLEDGEMENTS

The author thanks the sponsors of CREWES for continuing support.

REFERENCES

Claerbout, J.F., 1983, Ground Roll and Radial Traces: Stanford Exploration Project Report, **SEP-35**, pp 43-53.

Henley, D.C. 2003, Coherent noise attenuation in the radial trace domain, Geophysics, **68**, No. 4, pp1408-1416.

Henley, D.C., 2004, Attenuating the ice flexural wave on arctic seismic data: CREWES Research Report, **16**.

Henley, D.C., 2001, Spectral clipping: a ProMAX module for attenuating strong monochromatic noise, CREWES Research Report, **13**.

Henley, D.C, 2011, Getting something for nothing—or not: interpolating coherent noise: CREWES Research Report, **23**.